

EXAMINING THE M/Z SEPARATIVE CAPABILITY OF TRAVELLING WAVES FOR LARGE MOLECULE CHARACTERISATION

Jakub Ujma,¹ David Langridge,¹ Keith Richardson,¹ Kamila Pacholarz,² Ellen Liggett,³ Jason Wildgoose,¹ Perdita Barran,³ Ian Anderson,⁴ Kevin Giles,¹ Malcolm Anderson¹

1. Waters Corporation, Wilmslow, United Kingdom; 2. KP is now an AstraZeneca employee, no further work presented here has been conducted using AstraZeneca resources, Manchester, United Kingdom; 3. University of Manchester, Manchester, United Kingdom; 4. Pharmaron Gene Therapy, Liverpool, United Kingdom

INTRODUCTION

Travelling wave (TW) induced ion transport in a gas depends on both mobility and m/z. The m/z dependence has been previously rationalised in terms of velocity relaxation times, which increase with m/z and wave velocity. As such, TW parameters can be tailored to yield separation dominated by m/z or mobility. Herein, we explore the use of TW devices to characterise the m/z and mobility of some high molecular weight species including the native monoclonal antibody (NIST mAb) and the empty and full capsids of adeno-associated virus (E:F AAV). We compare the TW data with those obtained using a linear field drift tube ion mobility (DTIM) device as well as ToF-MS to delineate m/z and mobility aspects of TW separations.

MATERIALS AND METHODS

The TW-based m/z separation was investigated on a SELECT SERIES™ Cyclic™ IMS and SYNAPT™ XS instruments (Figure 1 A and B) which feature TW ion mobility separators (TWIM) in a Q-TWIM-ToF-MS geometry. The TWIM device in the SYNAPT XS instrument was then replaced with a DTIM separator to allow “pure mobility” separations for comparison. Samples of full and empty AAV8 (UNC Vector Core, Lake Pharma), full and empty AAV5 and NIST mAb (Waters) were infused using nanoESI emitters (PicoTip™, New Objective). In order to activate and unfold mAb ions, cone voltage of 150V and trap collision energy of 80 eV was applied. All samples were desalted (Micro Bio-Spin™ 6) and dissolved in 150 mM ammonium acetate. In order to explore the m/z dependence on TW separation, data were acquired at different ratios of TW amplitude and velocity. Experimental results were correlated with analytical models and ion-trajectory simulations (SIMION).

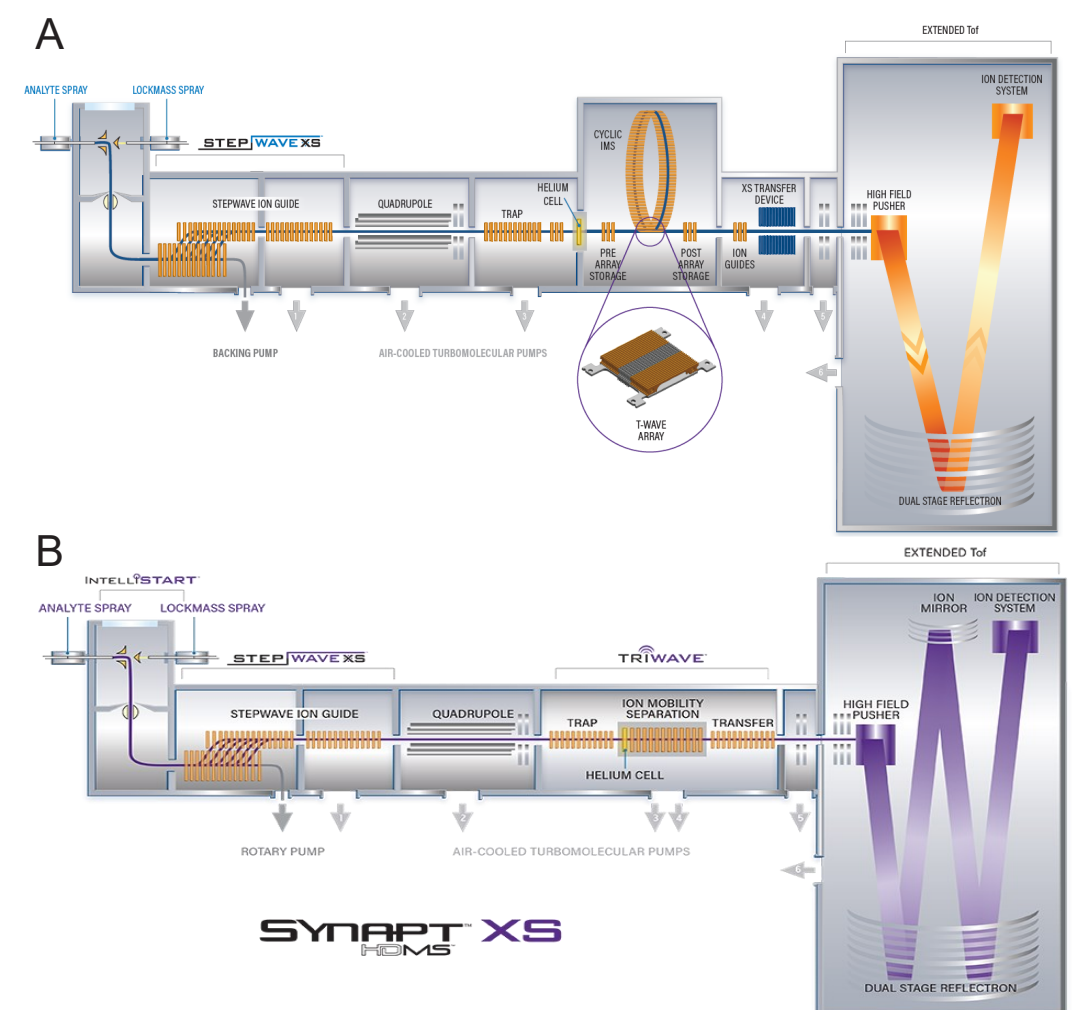


Figure 1. Instruments used in this study. A: SELECT SERIES Cyclic IMS. B: SYNAPT XS. For the DTIM work, the TWIM cell in the SYNAPT XS was replaced with Linear Field Drift Tube.

VELOCITY RELAXATION

Unlike in DTIM spectrometry, where ions drift through the gas at their terminal velocities, the travelling wave (TW) induced ion transport involves a perpetual cycle of acceleration and deceleration, as ions are being pushed and overtaken by the TWs. During each cycle, ions will approach (but never reach) the drift velocity dictated by their mobility (K). This “velocity relaxation” effect has been encountered in the past, notably in the “field reversing” experiments of Johnsen and Biondi¹ who correlated the relaxation time to the product of an ions’ m/z and K. The weak m/z dependence of TWIM separations has been known about for some time. Normally considered disadvantageous, it is typically circumvented via calibration approaches aiming to extract K from TW transit times.² Recently, Richardson *et al.* have considered m/z effects in smoothly-moving TW separations.^{2,3} For a given ion and a chosen set of parameters, separation characteristics of the TW device were conveniently described in terms of the dimensionless parameters α and γ :

$$\alpha = 2\pi K \frac{v}{\lambda z} \quad \gamma = 2\pi K \frac{V_0}{v\lambda} \quad (1)$$

For sufficiently small α , velocity relaxation effects are negligible and average ion velocity is given by:

$$\bar{v} = v(1 - \sqrt{1 - \gamma^2}) \quad (2)$$

where V_0 is the applied TW amplitude, v is the TW velocity, λ is the TW wavelength. For all α and sufficiently small γ , the average ion velocity is given by equation 3:³

$$\bar{v} = \frac{v}{1 + \alpha^2} \left[\frac{\gamma^2}{2} + \frac{\gamma^4}{8} \frac{1 + 10\alpha^2 + 15\alpha^4}{(1 + \alpha^2)^2(1 + 4\alpha^2)} + \frac{\gamma^6}{16} \frac{1 + 23\alpha^2 + 234\alpha^4 + 1171\alpha^6 + 2291\alpha^8 + 1620\alpha^{10}}{4(1 + \alpha^2)^4(1 + 4\alpha^2)^2(1 + 9\alpha^2)} \right] \quad (3)$$

It has been shown² that real TW devices can be calibrated by rescaling α and γ using new parameters a and g . This calibration is TW velocity dependent, but a and g are strongly linearly correlated. It should therefore be possible to extend the existing calibration protocol² to allow m/z determination. Further measurements using standards will be required to validate this approach.

For any combination of operating parameters and ion properties (i.e. α and γ), one can calculate the % reduction in ion velocity caused by velocity relaxation (Figure 2) and thus estimate the magnitude of the contribution of m/z and K on the TW transit time. The symbols show α , γ and the % reduction in velocity, calculated for all the ion species analysed in this study.

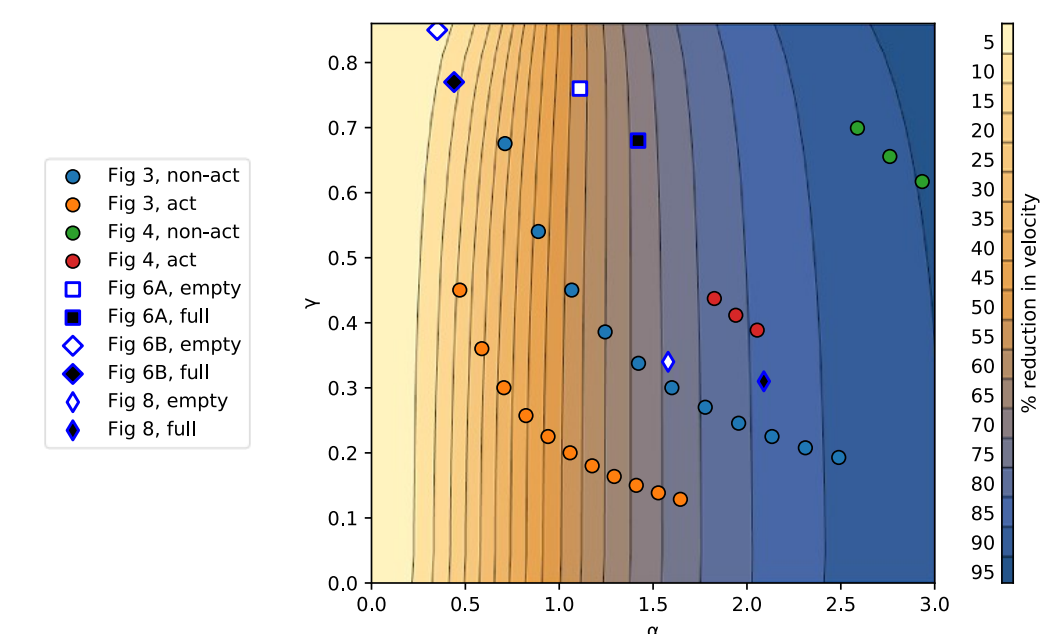


Figure 2. The percentage reduction in particle velocity caused by velocity relaxation as a function of α and γ in a smoothly-moving TW device. The symbols represent all the datasets included in this study.

TW BASED M/Z SEPARATION OF ANTIBODY CHARGE STATES

To highlight the transition from mobility dominated separation towards the m/z dominated regime, we present Cyclic IMS data obtained on non-activated and activated mAb ions acquired at a TW height of 45 V, a pressure of 1.8 mbar and a range of TW velocities (Figure 3A and B). The arrival time distributions (ATDs) of non-activated ions (blue traces) show distinct peaks at TW velocity of 600 m/s, these peaks correspond to charge states as evident from Figure 3B. The activated ions present as a broader profile, with three resolved features at low TW velocities. As the % of velocity relaxation increases (see Figure 2, blue and orange sets) these features shift and ultimately merge, while the separation between ATDs of individual charge states increases. Resolved charge state peaks are seen at 1300 m/s and overlap with those of non-activated ions. Interestingly, at TW velocities of 1400 m/s and above, we observe a reversal of arrival time (i.e. the activated ions have a shorter arrival time than the non-activated). This is not predicted by smoothly-moving TW theory and needs further investigation.

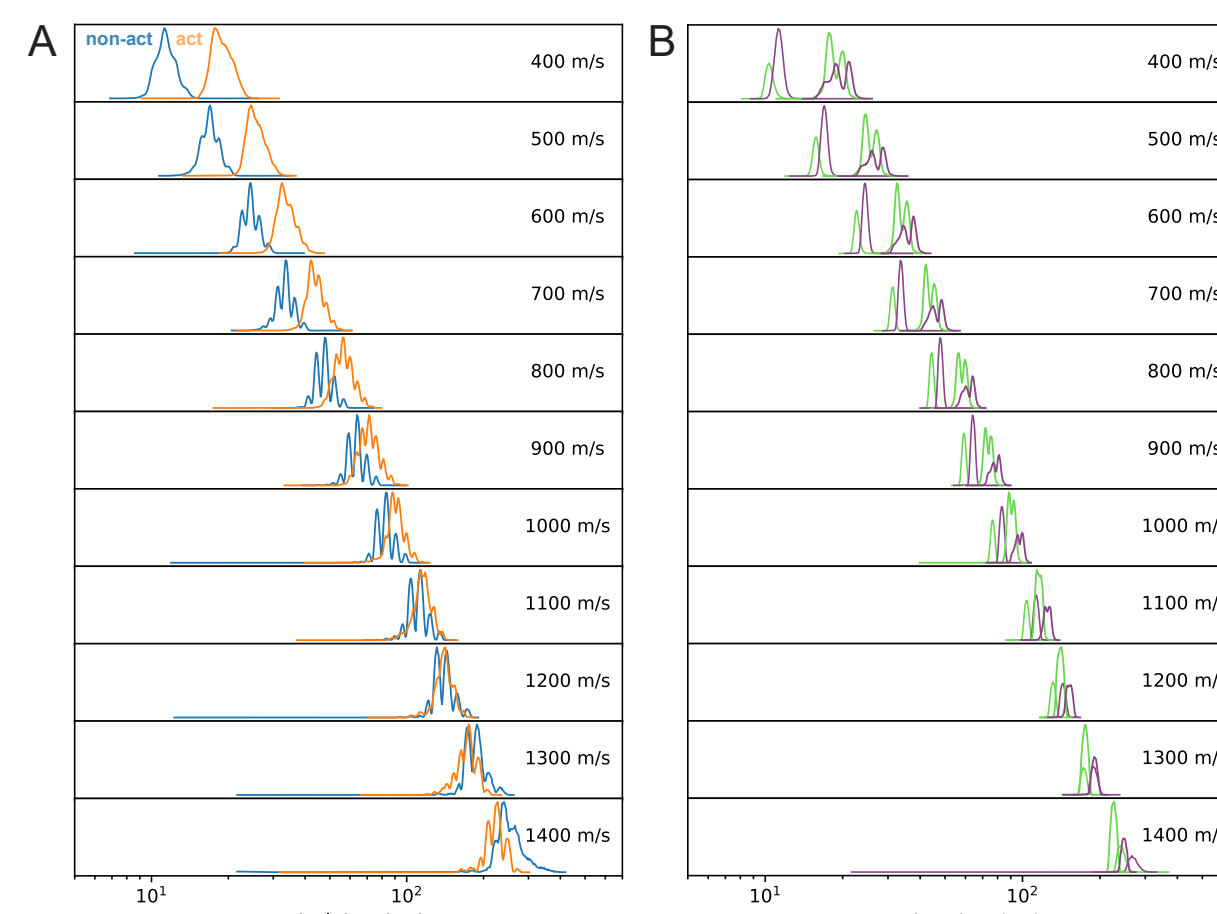


Figure 3. Arrival time distributions (ATDs) of mAb ions recorded at varying TW velocities, TW height of 45V and pressure 1.75 mbar (note the log arrival time scale). A: ATDs of all charge states. B: ATDs of selected charge states (green: 26+, purple: 25+).

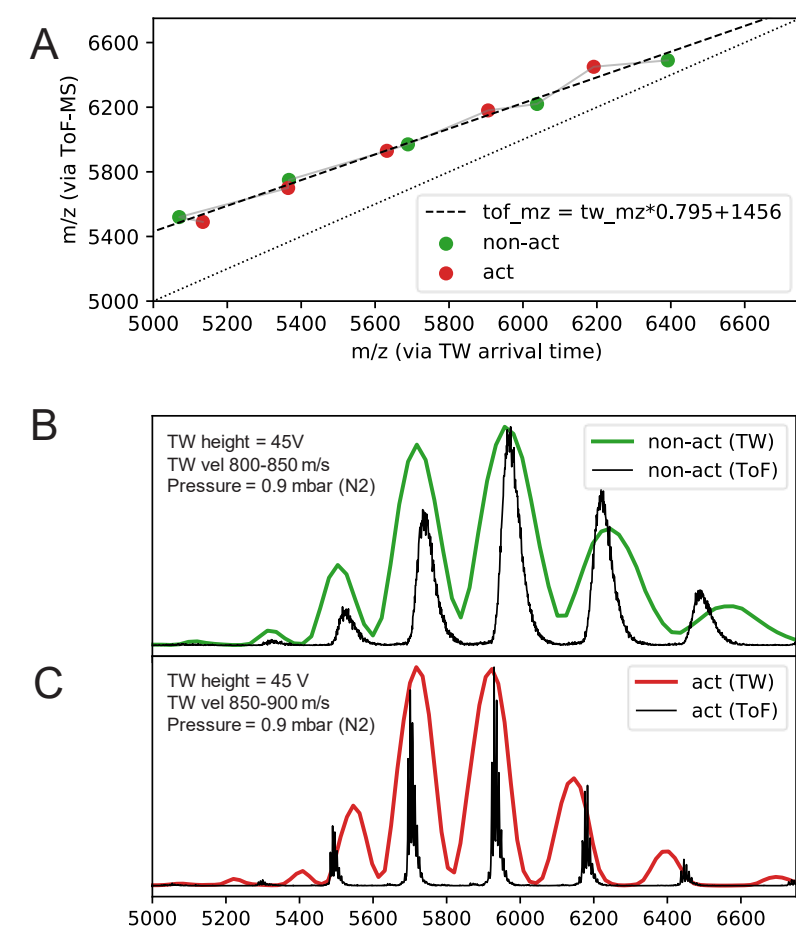


Figure 4. mAb m/z data recorded via TW (1 pass, green and red) and ToF-MS (black). A: Correlation between m/z values measured using ToF-MS and the predictions from equation 3 (see main text for details). B, C: Non-act and act ATDs plotted on a common m/z axis following calibration via equation shown in A.

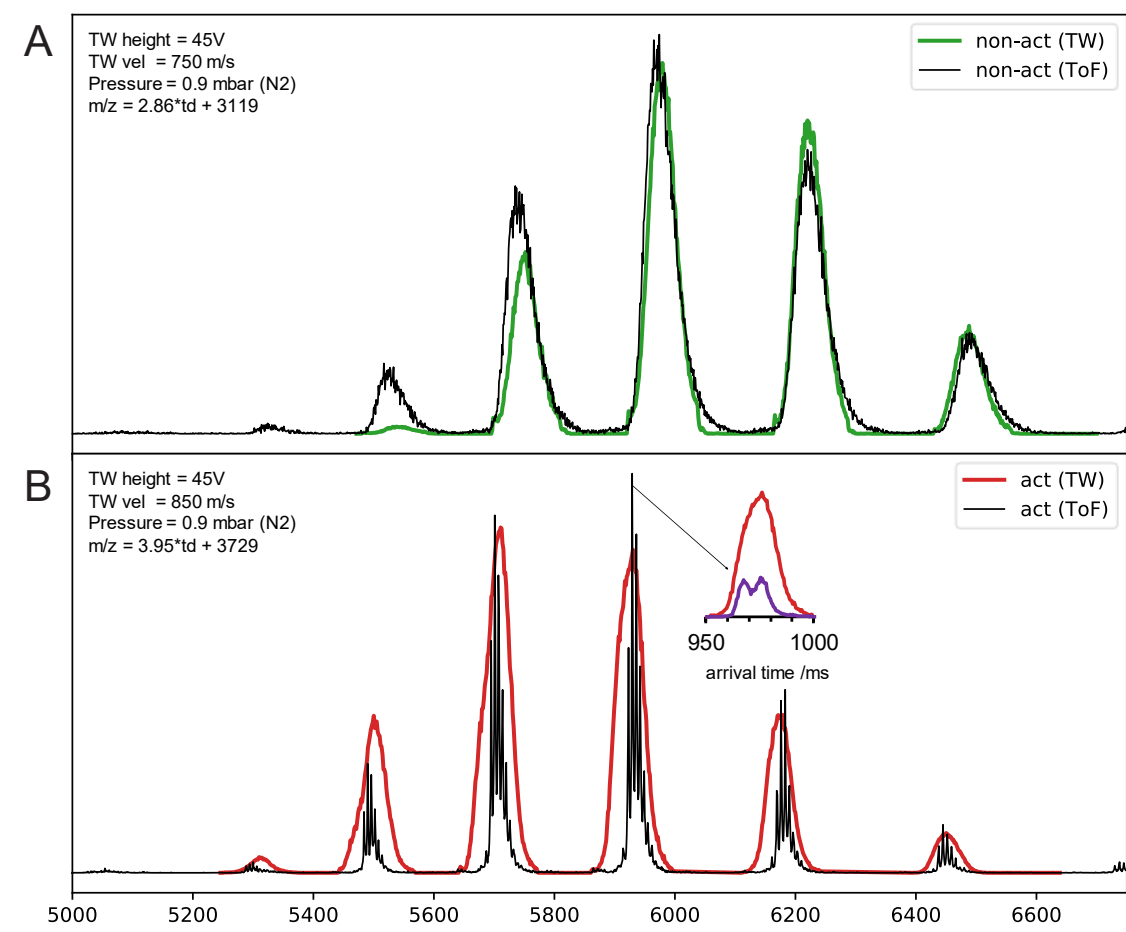


Figure 5. Multi-pass TW-MS data obtained on non-activated (green) and activated (red) mAb ions. Ions of each charge state were mass selected using the quadrupole and subjected to 20 passes around the cyclic ion guide. The corresponding MS data are shown in black.

TW BASED M/Z SEPARATION OF EMPTY AND FULL AAV CAPSIDS

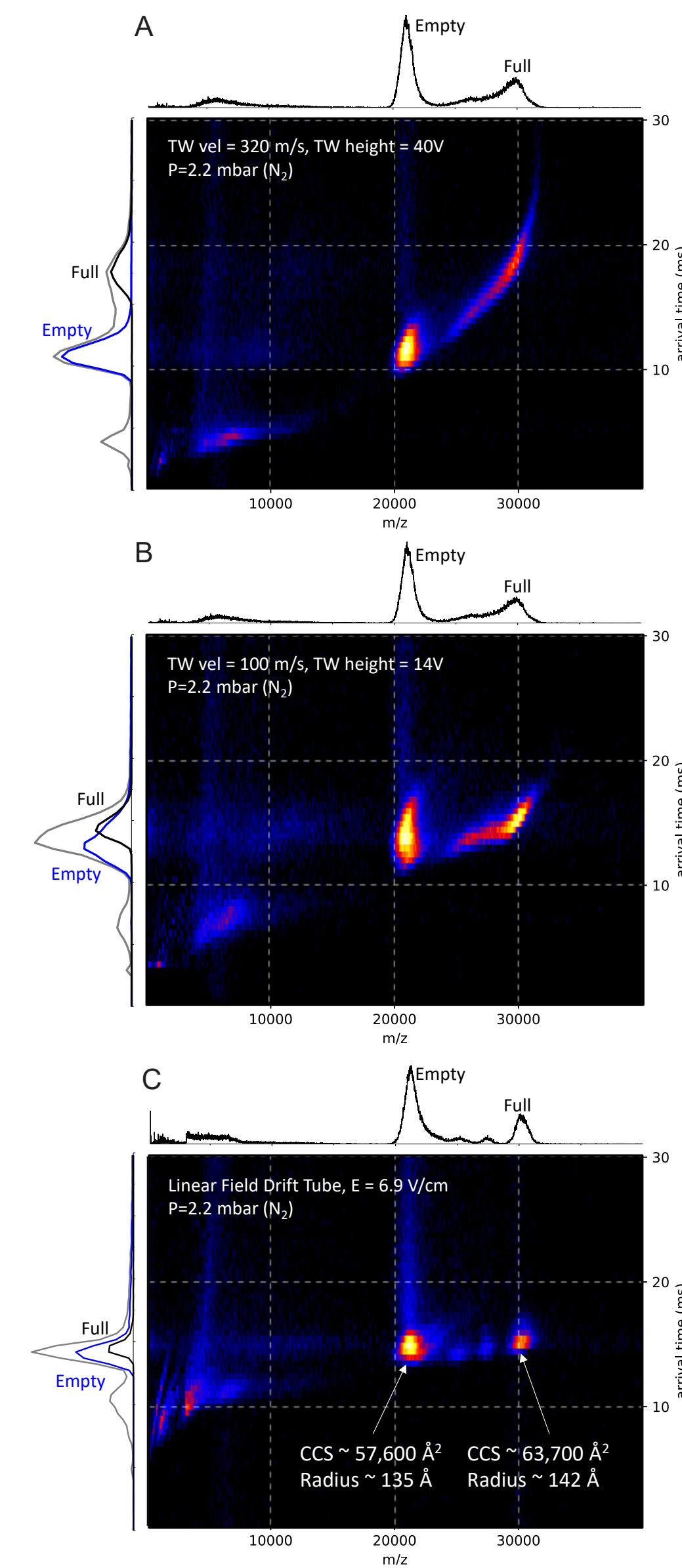


Figure 6. Full and Empty AAV5 data recorded on SYNAPT XS. A: TW conditions resulting in m/z dominated ion transport. B: TW conditions resulting in mobility dominated ion transport. C: Corresponding data acquired using Linear Field Drift Tube, pure mobility - drift time dependence. CCS values calculated assuming masses of 3.6 and 5.1 MDa and average charge of 170.

Characterization of the ratio of full-genome-containing, partially filled and empty capsids of adeno-associated virus is a major analytical challenge in gene therapy development. The high degree of structural heterogeneity of AAV precludes observation of individual charge states, however since both full and empty particles carry a similar average charge they are distinguishable by m/z.⁴ Here, we show the separation of full and empty AAV capsids by ToF-MS and a TW device (SYNAPT XS TW cell, ~25 cm long) set up either to maximise the m/z effect (higher α , Figure 6A) or to provide K dominated ion transport (lower α , Figure 6B). The same sample was also analysed using a DTIM device where only K-based separation is present (Figure 6C). These data indicate that empty and full capsids would be difficult to separate using DTIM, but by introducing more m/z-based separation, they can be separated using TWs. Preliminary CCS values (and radii) determined via DTIM are in agreement with data obtained from CryoEM.⁵ Single pass Cyclic IMS (98 cm) highlights better TW separation of full and empty AAVs (Figure 7A) and suggests the ability to distinguish partially filled capsids, similarly to ToF-MS (Figure 7B).

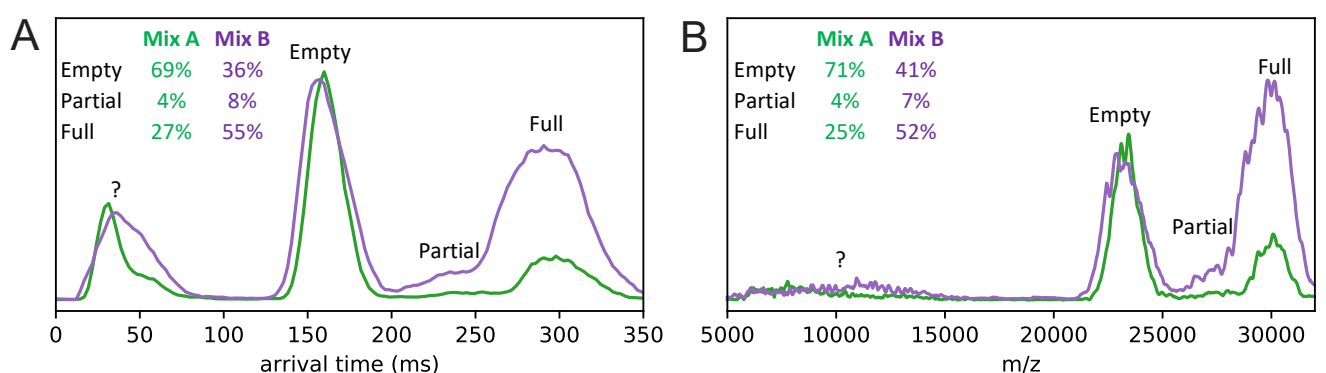


Figure 7. AAV8 data (two mixes) recorded on the Cyclic IMS instrument. A: separation of capsid forms in the Cyclic TW device. B: separation of capsid forms in the ToF-MS.

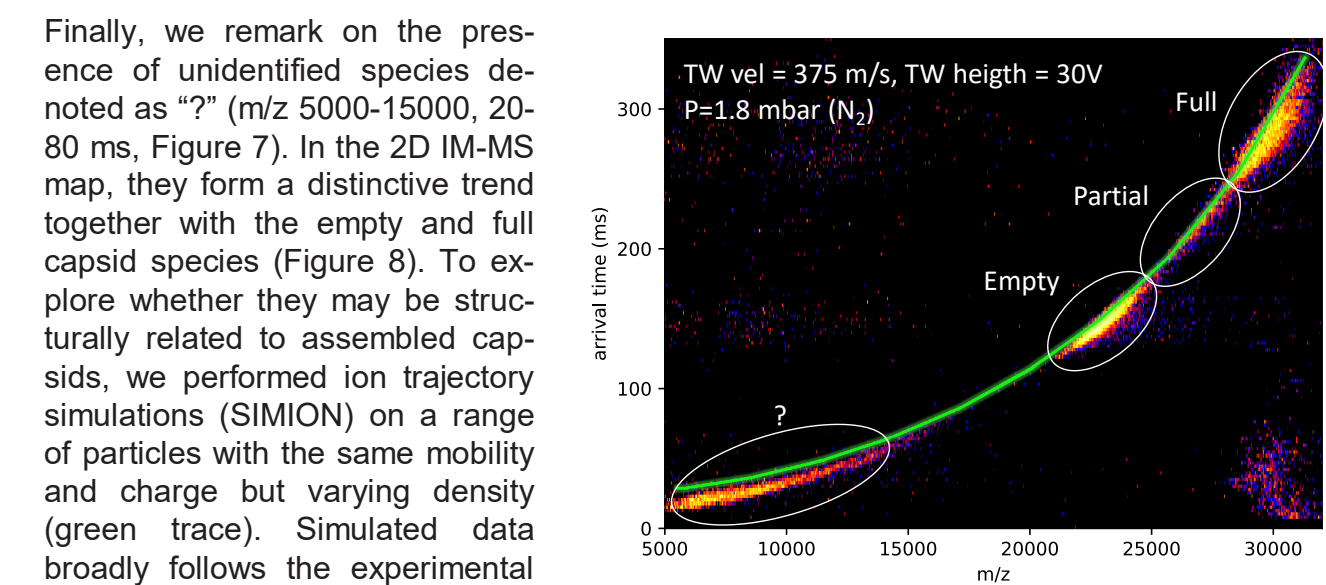


Figure 8. Full and Empty AAV8 data recorded on Cyclic IMS. Green trace: SIMION simulation results for a range of hypothetical capsids with constant K and charge but varying density.

SUMMARY AND OUTLOOK

- Demonstrated feasibility of m/z separation using a TW device operating at mbar pressure.
- TW based m/z separation of mAb charge states allows for rudimentary mass measurement.
- TW based m/z separation of empty and full AAVs allows for determination of their relative amounts.
- Future work will explore the TW-MS calibration approaches.

References

1. Johnsen, R.; Biondi, M. A. *J. Chem. Phys.* 1972, 57 (5), 1975–1979
2. Richardson, K.; Langridge, D.; Dixit, S. M.; Ruotolo, B. *Anal. Chem.* 2021, 93 (7), 3542–3550
3. Richardson, K.; Langridge, D.; Giles, K. *JMS* 2018, 428, 71–80
4. Pierson, E. E.; Keffler, D. Z.; Asokan, A.; Jarrold, M. F. *Anal. Chem.* 2016, 88 (13)
5. Silveria, M.A.; Large, E.E.; Zane, G.M.; White, T.A.; Chapman, M.S. *Viruses* 2020, 12, 1326.